

# A practical image reconstruction and processing method for symmetrically off-center detector CBCT system

HAO Jia<sup>1,2</sup> ZHANG Li<sup>1,2,\*</sup> LI Liang<sup>1,2</sup> CHEN Zhiqiang<sup>1,2</sup> KANG Kejun<sup>1,2</sup>

<sup>1</sup>Department of Engineering Physics, Tsinghua University, Beijing 100084, China

<sup>2</sup>Key Laboratory of Particle & Radiation Imaging (Tsinghua University), Ministry of Education, Beijing 100084, China

**Abstract** CBCT scanners have been widely used in angiography, radiotherapy guidance, mammography and oral maxillofacial imaging. To cut detector size, reduce manufacturing costs and radiation dose while keeping a reasonable FOV, the flat panel detector can be placed off-center horizontally. This scanning configuration extends the FOV effectively. However, each projection is transversely truncated, bringing errors and artifacts in reconstruction. In this paper, a simple but practical method is proposed for this scanning geometry based on truncation compensation and the modified FDK algorithm. Numerical simulations with jaw phantom were conducted to evaluate the accuracy and practicability of the proposed method. A novel CBCT system for maxillofacial imaging is used for clinical test, which is equipped with an off-center small size flat panel detector. Results show that reconstruction accuracy is acceptable for clinical use, and the image quality appears sufficient for specific diagnostic requirements. It provides a novel solution for clinical CBCT system, in order to reduce radiation dose and manufacturing cost.

**Key words** Cone beam CT, Off-center detector, Image reconstruction, Field of view, Projection truncation, Central artifacts

## 1 Introduction

With the rapid development of CT technique, cone beam CT (CBCT) based on volumetric tomography has brought a revolution for radiation imaging, especially angiography, radiotherapy guidance, mammography, and oral maxillofacial imaging. Compared with conventional multi-slice CT (MSCT), the CBCT system has many significant advantages, such as smaller size, smaller radiation dose, and lower cost. Also, the CBCT cuts the examination time, reduces image unsharpness caused by the translation of the patient and image distortion due to internal patient movements<sup>[1]</sup>. Flat panel detectors used in CBCT systems increase X-ray absorption efficiency<sup>[2]</sup>.

Compared with the MSCT, the CBCT system has its own disadvantages. One is the low image quality related to noise and contrast resolution because of the detection of large amounts of scattered

radiation<sup>[3]</sup>. Another one is the limited field of view (FOV), which usually causes projection truncation. Generally, the FOV dimensions, likely covered by CBCT, depend primarily on the detector size and shape, the beam projection geometry, and the ability to collimate the beam<sup>[4]</sup>. To reduce manufacturing costs, the smaller size detector is always required. In this paper, a novel CBCT scanning geometry to extend the FOV width of is studied by offsetting the position of the detector, collimating the beam asymmetrically, and scanning only half the object in each angle position. In this case, the projections are transversely truncated, leading to serious truncation artifact and value error by traditional reconstruction method.

In circular orbit CBCT system, the FDK reconstruction algorithm is widely used because of several advantages including simple mathematical equation, quick computation, and easy implementation etc<sup>[5]</sup>. However, the traditional FDK algorithm requires that the projection data were not truncated in

Supported by National Key Technology R&D Program of the Ministry of Science and Technology (No.2012BAI07B05).

\* Corresponding author. E-mail address: zli@mail.tsinghua.edu.cn

Received date: 2012-09-20

horizontal direction, or it will result in serious errors and truncation artifacts. Many attractive algorithms have been suggested over the years for projection truncation problems. Cho *et al.*<sup>[6]</sup> proposed the pre-weighting and post-weighting FDK algorithms mitigating the truncation artifacts to a certain degree. Zamyatin *et al.*<sup>[7]</sup> adapted the similar concept of approximating truncated data by complementary rays for helical CT with off-center detector. In 2004, Noo *et al.*<sup>[8]</sup> reported a two-step Hilbert transform method for parallel-beam and fan-beam image reconstruction from transversely truncated projections according to Zou and Pan's work<sup>[9]</sup>. Also, this BPF-type reconstruction algorithm based on PI-line has been expanded to exact reconstruction within ROI from reduced-scans data containing transverse truncations. In the off-center detector scanning scenario, the BPF reconstruction methods give the good results. Leng *et al.*<sup>[10]</sup> applied a BPF algorithm to the fan-beam case of an asymmetric half-size detector. Li *et al.*<sup>[11,12]</sup> reported a BPF-type reconstruction algorithm to cone-beam CT system with a reduced size detector positioned off-center. Besides FDK and BPF algorithms, algebraic and statistical maximum-likelihood reconstruction algorithms have been used in off-center detector CT reconstruction, handling the native truncated cone-beam projection data and improve image quality<sup>[13]</sup>. Still, the high computation load is a major challenge to their clinical use in the CBCT imaging.

However, the clinical application of the off-center detector CBCT system is still confronted with a lot of problems, one of the most problems is to reduce the artifacts brought by small size detector and ensure the correct of reconstructed value<sup>[14]</sup>. In this paper, we investigate the off-center detector CBCT scanning geometry and reconstruction method. Motivated by the idea proposed by Cho *et al.* in Ref.[6], a simple but practical solution is proposed based on truncation compensation and the modified filtered back-projection (FBP) method, and its feasibility is demonstrated by numerical studies. A novel oral CBCT system with off-center small size flat panel detector was designed for maxillofacial imaging, and clinical experiments were conducted.

## 2 Materials and methods

### 2.1 System geometry

In the CBCT system, an X-ray tube and flat panel detector are fixed to a rotating gantry. During the rotation, multiple sequential planar projection images of the FOV as projection data are acquired. The CBCT system can theoretically reduce the completeness of the scanning trajectory and still reconstruct a 'short scan'<sup>[15]</sup>. To complete data set, a full scan of 360° is needed using off-center detector scanning geometry.

In Fig.1(a), a small size and off-center detector is placed symmetrically, covering only half of the scanning object in each scanning angle. The scanning plane ( $O', x, y$ ) is central.  $S$  is the X-ray source, and  $R$  is the scan trajectory radius. The width and height of the flat panel detector are along  $a$  and  $b$  axis. 3-D projections from the flat panel detector is represented as  $p(\phi, a, b)$  in Fig.1(b), here,  $\phi$  is the rotation angle. Attenuation information reconstructed from the projections is represented as  $f(x, y, z)$  centered on the origin  $O'$  of a Cartesian coordinate system. Scanning parameters in the simulation and experiment are shown in Table 1, indicating that a smaller size can achieve a larger transverse FOV, this is useful in cost and dose reduction.

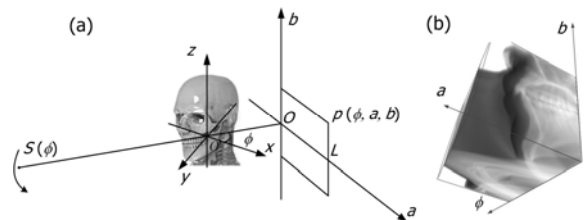


**Fig.1** (a) Scanning geometry of oral CBCT with symmetrically off-center small size detector. (b) Projection data from the small size detector CBCT.

**Table 1** System configuration of CBCT in the numerical study and the practical experiments

System configurations	Parameters
Distance from source to detector / mm	750
Distance from source to rotation center / mm	500
Detector size / mm×mm	130×130
Detector pixel number	512×512
Detector pixel size / $\mu\text{m}$	254
Scan angle	360°
Projections per scan	360

## 2.2 Reconstruction method

In Fig.1(b), projection in each angle view ( $\phi$ ) is truncated transversely. This truncation will produce a sharp-cut boundary, and its Fourier representation manifests as oscillating ripples and overshoots around the boundary, as described by the Gibbs effect. The Gibbs effect and truncation artifacts can be reduced by extrapolating the truncation boundary under a continuous and smooth condition. The different padding methods have been proposed<sup>[16-18]</sup>, and cause the reconstructed CT numbers to deviate from the truth, or the projection estimation process is too complex to commercially apply.

In the two-dimensional condition (fan-beam CT scanning), when the detector is off-center, data completeness conditions for an exact and stable reconstruction can be satisfied with a full scan of  $360^\circ$ <sup>[19]</sup>. The standard projection data can be obtained by establishing the relationship between the missing rays and opposite rays. This process is called as ‘rebinning’ and the reconstruction is exact theoretically<sup>[20]</sup>. In cone-beam reconstruction, the circular data acquisition does not yield a complete set of the three-dimensional radon values, thus achieving only approximate reconstruction. A similar padding method can be used to approximately estimate the truncated projection by off-center detector. The missing half of the projections are filled with the nearest opposing rays slice by slice as Eq.(1).

$$p_{\text{estimate}}(\phi, a, b) = p(\phi + \pi \pm 2\beta, -a, b) \quad (1)$$

Then, extrapolated projections is obtained by

$$\tilde{p}(\phi, a, b) = \begin{cases} p(\phi, a, b), & a \geq 0 \\ p_{\text{estimate}}(\phi, a, b), & a < 0 \end{cases} \quad (2)$$

This estimation is not accurate outside the middle plane. Errors increase with the growth of cone angle, and a sudden discontinuity can splice the real and estimated data. It should be smoothed to avoid artifacts in reconstructed images. The convolution with a Gaussian function is applied to the region of  $a \in [-\Delta, \Delta]$  in the fixed projection to make left and right part link together smoothly. In the following study,  $\Delta$  is set to 12 pixels.

This method provides the closest data available to estimate the missing projection. The spliced datasets

can only use as filtering and keeping numerical inaccuracy in the reconstruction volume, and perform better than cosine extrapolation, constant extrapolation, linear extrapolation and the other methods in numerical accuracy. After projection estimation, full length projection data are obtained. After filtering, only the measured data are used in the back-projection procedure to form the reconstruction volume. Reconstruction is summarized as follows.

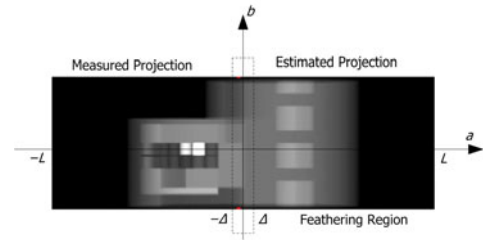


**Fig.2** Projection image after estimation and smoothing in an angle view. The left part is measured by off-center detector; and the right, the estimation method in the section of 2.1. The region of  $[-\Delta, \Delta]$  is used for image smoothing.

The projection depends on the fan-angle and the cone-angle is weighted by a pre-weighting factor. Convolution with the ramp-filter  $g^p(a)$  is applied.

$$\tilde{p}(\phi, a, b) = \left( \frac{R}{\sqrt{R^2 + a^2 + b^2}} \tilde{p}(\phi, a, b) \right) \times g^p(a) \quad (3)$$

Then, the pre-weighted and filtered projections are back-projected into the reconstruction volume over the complete angle interval of  $360^\circ$ . After filtering, the measured part ( $a > 0$ ) in the fixed projection is back-projected to form the reconstruction, to avoid artifacts induced by inaccurate projection extrapolation.

$$f(x, y, z) = \int_0^{2\pi} \frac{R^2}{U(\phi, x, y)^2} \tilde{p}(\phi, a, b)|_{a>0} d\phi \quad (4)$$

The  $1/[U(\phi, x, y)^2]$  in Eq.(4) is identical in fan-beam back-projection.

$$U(\phi, x, y) = R + x \cos \phi + y \sin \phi \quad (5)$$

In the scanning path plane, the missing part is recovered exactly as FDK. Due to cone angle and data missing, the truncated part cannot be fixed exactly in the other planes. There is discontinuance in the boundary between the original and estimated projections. Errors are expected to increase away from the middle plane with growth of cone angle. So, the artifact reduction after reconstruction is needed.

### 2.3 Central artifacts reduction

In the reconstructed coronal slices, the artifact as a circular region near the rotation center with abnormal intensity variation is obvious. Left-right intensity imbalance in the central coronal slices is observed. Besides the errors in truncated estimation, there is the scatter for reconstruction artifact. In the experiments with an offset scanning geometry, the scatter asymmetric distribution leads to the obvious central artifact, especially around the central axis of the reconstructed imaging FOV<sup>[21]</sup>. Accurate scatter estimation and post-processing scatter reduction can reduce the central artifacts. However, this needs to be conducted by Monte Carlo simulation, and followed by an iterative fitting process. For this method, simulating complex objects is difficult and computationally expensive<sup>[22]</sup>.

The image post-processing in the reconstructed volume is practical for reducing central artifact. Here we use a bicubic interpolation method in its central area. The selected central area in each transaxial plane is replaced by bicubic interpolation data, and smoothed by a 3D Gaussian filter, then the central artifacts is reduced to a certain extent. In oral imaging, the central artifact has little impact on the diagnosis as we focus on the teeth and jaw. Thus, a simple processing is enough for clinical application.

## 3 Experimental and simulation

### 3.1 Simulation

In order to provide a stringent and realistic test for the proposed method, a mathematical 3D jaw phantom with varying contrast levels is used as the simulation studies, thus evaluating the reconstruction performance and displaying the most important structures in the jaw region with a minimal number of simple geometrical objects<sup>[23]</sup>. Three molars are replaced by crowns of the high densities, in order to observe the influence of metal artifacts. Projections are obtained by a flat panel detector. In each scan, the total number of projection views is 360 over a full 360° circle around the jaw phantom. The reconstructed volume size is 512×512×512. Scanning geometry is the same as Fig.1.

In the reconstructed volume (Fig.3), the different slices are reconstructed by conventional FDK method from a full-size detector CBCT scanning and the proposed method from a half-size detector CBCT scanning. All the images are shown in the same gray scale of [0.5, 3]. The results demonstrate that the proposed method is available to reconstruct volume image for off-center half-size detector CBCT system, and can avoid truncated artifacts. There is no severe reconstruction difference from full-size FDK method and the proposed method. However, the streak artifacts in the presence of high-contrast objects are more severe in the second slice. The reconstructed gray-scale profiles of transaxial slices are shown in Fig.4, indicating that the density deviations from full length detector data and off-center detector data are similar in the reconstructed results, and the proposed method can save detector size, and reconstruct the object correctly.

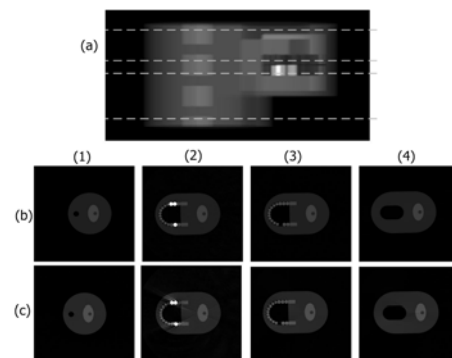


**Fig.3** Reconstructed images. (a) Projection image of FORBILD jaw phantom, the additional dashed lines show the location of the planes investigated in (b) and (c). (b) Reconstructed planes of the FORBILD jaw phantom from full-size detector projections with FDK method. (c) Reconstructed planes of the FORBILD jaw phantom from half-size detector projections with the proposed method in Section.2.

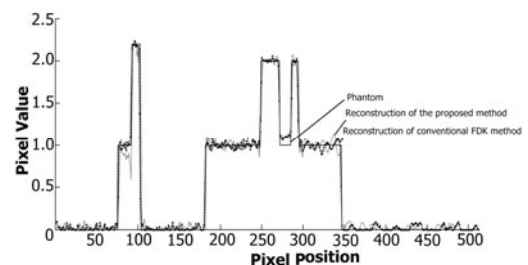


**Fig.4** Central gray-scale profiles within the plane (2) in the reconstructed images between the true phantom values. The FDK result from a full-size detector CBCT scanning and the proposed method from the half-size off setting detector CBCT scanning.

For quantitative comparison, we use NMSD (Normalized Root Mean Squared Distance) as an evaluation standard. It is defined as Eq.(6).

$$r_{\text{NMSD}} = \left( \frac{\sum_{i,j} (f(x,y) - f_R(x,y))^2}{\sum_{i,j} (f_R(x,y) - f'_R(x,y))^2} \right)^{0.5} \quad (6)$$

Here  $f_R$  is the reference image and  $f'_R$  is its mean value. The average NMSD in different slices of full size detector is  $0.92 \times 10^{-4}$ ; and  $1.13 \times 10^{-4}$ , the proposed method from half-size detector. The reconstructed value is more accurate than the other extrapolation methods, and acceptable for clinical application, especially in dental imaging and IGRT.

### 3.2 Experimental

Using high-contrast FORBILD jaw phantom, the objects can be accurately reconstructed by the proposed method from a half-size detector. However, the scanning object in clinical practice is far more complicated than the phantom. Therefore, we conducted the clinical oral scanning data. Experiments were carried out on a novel experimental CBCT system designed for maxillofacial imaging with a 13 cm×13 cm flat panel detector. By off-centered the detector, the FOV achieves 15 cm×8 cm and covers the maxillofacial region. In the experiments, the X-ray tube works at a voltage of 100 keV and the X-ray tube current was 3 mA. Total projection number is 360. The rotation and data acquisition time is about 20 s/scanning. The reconstructed transaxial and sagittal planes are shown in Fig.5. It can be found that the proposed method has the ability to reconstruct fine detailed high-contrast structures from off-center detector CBCT system and remove truncation artifacts. In general, the image quality and reconstruction accuracy meet the clinical requirements, especially oral and maxillofacial imaging. As shown in Figs.(5) and (6), the image quality is acceptable due to removing the truncation artifacts.

There is a trade-off between the signal-to-noise ratio (SNR) and projection amount. Compared with the full size detector configuration, the SNR is impacted because of reducing projection data by half, and the streak artifacts are more severe in the presence of high-contrast objects. This can be reduced by image

processing methods after reconstruction. In view of the dose and cost reduction, this is practical and useful.

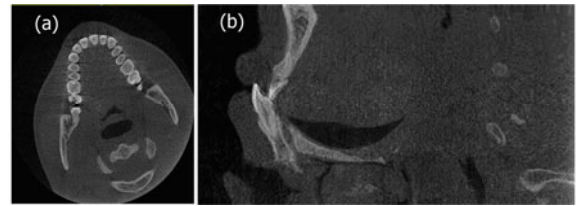


**Fig.5** Real data reconstruction results from an off-center detector in dental CBCT system. (a) the middle transaxial plane, (b) the sagittal plane.



**Fig.6** Three-dimensional representation of the reconstructed volume from a half-size off-center detector CBCT system.

## 4 Discussion

This method is demonstrated by clinical study. Future enhancements likely direct to improve image quality and reduce the noise disturbance. New reconstruction algorithms will focus on the dose benefits and high image qualities, such as algebraic reconstruction technique and statistical iterative reconstruction algorithms. In the CBCT system, the poor soft tissue contrast is another challenge, and the scattered radiation is significant factor in reducing the contrast.

## 5 Conclusion

In this paper, a novel circular CBCT scanning configuration with off-center detector is introduced. It effectively saves detector size, reduces the manufacturing cost and radiation dose, and extends the transverse FOV. A process method based on truncation compensation and the modified FDK-type algorithm is proposed, and its effectiveness is demonstrated by numerical simulation and experiment. The reconstruction accuracy is acceptable for clinic and the image quality is sufficient for specific diagnostic requirements. Also, this method has high computation efficiency and easy implementation for commercial application. Using GPU acceleration technique, the

volume can be reconstructed from raw projection data in half a minute. The central artifact is reduced by image process after reconstruction, impacting the diagnosis. However, using this scanning geometry the SNR of reconstructed image will be degraded, as the detector size is reduced. In the future, noise reduction methods will be studied, to improve the image quality.

## References

- 1 Zhang K, Li M, Dai J, *et al.* Nucl Sci Tech, 2011, **22**: 111–117.
- 2 Liang X, Jacobs R, Hassan B. Eur J Radiol, 2010, **75**: 265–269.
- 3 William C S, Allan G F. Dent Clin North Am, 2008, **52**: 707–730.
- 4 Zhang X Z, Qi Y J. Nucl Sci Tech 2011, **22**: 338–343.
- 5 Feldkamp L A, Davis L C, Kress J W. J Opt Soc Am, 1984, **1**: 612–619.
- 6 Cho P S, Ruddt A D, Johnson R H. Comput Med Imag Grap, 1996, **20**: 49–57.
- 7 Zamyatin A A, Taguchi K, Silver M D. Med Phys, 2005, **32**: 3117–3127.
- 8 Noo F, Clackdoyle R, Pack J D. Phys Med Biol, 2004, **49**: 3903–3923.
- 9 Zou Y, Pan X. Phys Med Biol, 2004, **49**: 941–959.
- 10 Leng S, Zhuang T, Nett B E. Phys Med Biol, 2005, **50**: 1805–1820.
- 11 Li L, Chen Z Q, Zhang L. High Energ Phys Nucl, 2006, **30**: 812–817.
- 12 Li L, Chen Z Q, Zhang L, *et al.* Nucl Sci Tech, 2006, **17**: 113–117.
- 13 Hansis E, Bredno J, Sowards E D, *et al.* Proc IEEE Nucl Sci Sym, 2010, 2228–2231.
- 14 Zamyatin A A, Nakanish S. Med Phys, 2007, **35**: 1593–1604.
- 15 Parker D L. Med Phys, 1982, **9**: 254–257.
- 16 Zhao S, Yang K, Yang X. J X-Ray Sci Technol, 2011, **19**: 155–172.
- 17 Hsieh J, Chao E. Med Phys, 2004, **31**: 2385–2391.
- 18 Sadowsky O, Lee J, Sutter G, *et al.* IEEE Tran Med Imaging, 2011, **30**: 69–83.
- 19 Li L, Chen Z Q, Wang G, *et al.* Nucl Sci Tech, 2005, **16**: 171–176.
- 20 Kak A C, Slaney M. Principles of Computerized Tomographic Imaging, IEEE Press, 1988.
- 21 Zhang G, Jacobs R, Nuyts J. Proc SPIE Med Imag, 2012, 83132U, 1–7
- 22 Jarry G, Graham S A, Moseley D J, *et al.* Med Phys, 2006, **33**: 4320–4329.
- 23 Watzke O. Jaw Phantom. <http://www.imp.uni-erlangen.de/phantoms/jaw/jaw.htm>